

See discussions, stats, and author profiles for this publication at: <https://www.researchgate.net/publication/231531823>

Residue-Specific pKa Measurements of the β -Peptide and Mechanism of pH-Induced Amyloid Formation

ARTICLE in JOURNAL OF THE AMERICAN CHEMICAL SOCIETY · SEPTEMBER 1999

Impact Factor: 12.11 · DOI: 10.1021/ja990864o

CITATIONS

72

READS

18

6 AUTHORS, INCLUDING:



Dale G Ray

Case Western Reserve University

19 PUBLICATIONS 925 CITATIONS

SEE PROFILE



Kurt Wollenberg

The Lubrizol Corporation

6 PUBLICATIONS 204 CITATIONS

SEE PROFILE



Michael G Zagorski

Case Western Reserve University

68 PUBLICATIONS 4,722 CITATIONS

SEE PROFILE

Residue-Specific pK_a Measurements of the β -Peptide and Mechanism of pH-Induced Amyloid Formation

Kan Ma,[†] Erin L. Clancy,[†] Yongbo Zhang,[†] Dale G. Ray,[†] Kurt Wollenberg,[‡] and Michael G. Zagorski^{*,†}

Contribution from the Department of Chemistry, Case Western Reserve University, Cleveland, Ohio 44106, and Lubrizol, Inc., 29400 Lakeland Boulevard, Wickliffe, Ohio 44092-2298

Received March 16, 1999

Abstract: The aggregation of the β -peptide into amyloid is a key pathological event in Alzheimer's disease. This process (β -amyloidosis) involves the conversion of soluble random coil, α -helical or β -sheet conformations into insoluble, aggregated β -pleated sheet structures. The pH is a significant extrinsic factor that influences β -amyloidosis, which must be related to the presence of ionizable groups in the β -peptide. To further evaluate this effect, we determined the dissociation constants (pK_a) of the side chains for the aspartic acid (Asp), glutamic acid (Glu), histidine (His), and tyrosine (Tyr) amino acid residues using NMR spectroscopy. The measurements were performed under different solution conditions, where the predominant conformation is either random coil or α -helix. We have used a peptide fragment that comprises residues 1–28 [β -(1–28)] of the natural β -(1–40) or β -(1–42) peptides, which is an appropriate model since the remaining 29–40 or 29–42 regions are devoid of polar and charged amino acid residues. The results demonstrate that the Glu and His residues have larger pK_a values in sodium dodecyl sulfate solution, suggesting that electrostatic interactions are important in stabilizing the α -helix and preventing an α -helix \rightarrow β -sheet rearrangement. A mechanism involving unfavorable interactions of the charged groups with the α -helix macrodipole is proposed for the pH-induced α -helix \rightarrow β -sheet transformation in water–trifluoroethanol solution.

Introduction

The major cause of adult-onset dementia is Alzheimer's disease (AD), a devastating disorder now affecting approximately 15 and 50% of the adult population in the United States over the ages 65 and 85, respectively.¹ The ultimate diagnosis of AD relies on an abundance of amyloid deposits in the brains of afflicted individuals. The major protein component of the amyloid deposits is the β -peptide, a small peptide composed of 39–42 amino acids. Recent studies demonstrated that the β -peptide becomes neurotoxic to cortical cell cultures when aggregated as amyloid-like β -sheet structures,^{2–4} thus establishing that this β -amyloidosis process is an important pathological event.

It is well-known that extrinsic or environmental factors such as the pH, peptide concentration, ionic strength, metal ions, membrane-like surfaces, and solvent hydrophobicity influence the relative proportions of the random coil, α -helix, and β -sheet solution structures and modulate the aggregation of the β -peptide into amyloid (random coil \rightarrow β -sheet or α -helix \rightarrow β -sheet).^{4–9} Many of these extrinsic factors could conceivably occur in brain microenvironments and thus may initiate β -amy-

loidosis. As a result, major research efforts are focused on uncovering a therapeutic procedure that stabilizes the α -helical or random coil structures, and thus prevent the β -peptide from precipitating into amyloid and becoming toxic to nerve cells.

The relative proportions of the solution structures, as well as the aggregation rates and fibril morphologies of the β -peptide, are highly pH dependent^{5,6,8–11} (Table 1). At acidic and basic pH, the β -peptide is mostly unstructured in aqueous solution, but becomes α -helical in membrane mimetic environments such as trifluoroethanol (TFE). At pH 4–7, the peptide produces aggregated β -sheet structure in water alone or water with TFE. We recently demonstrated large structure variations with pH and the charge of a micelle headgroup, in that charged micelles stabilize the α -helical structure over a wide pH range.¹² Taken together, these results demonstrate that the protonation states of the ionizable side-chain groups are important factors in β -amyloidosis.

To better understand the relationship between structure and the side-chain ionization states, we determined the site-specific

* To whom correspondence should be addressed. Phone: 216-368-3706. Fax: 216-368-3006. E-mail: mxz12@po.cwru.edu.

[†] Case Western Reserve University.

[‡] Lubrizol, Inc.

(1) Selkoe, D. J. *Trends Cell Biol.* **1998**, *8*, 447–453.

(2) Simmons, L. K.; May, P. C.; Tomaselli, K. J.; Rydel, R. E.; Fuson, K. S.; Brigham, E. F.; Wright, S.; Lieberburg, I.; Becker, G. W.; Brems, D. N.; Li, W. *Mol. Pharmacol.* **1994**, *45*, 373–379.

(3) Pike, C. J.; Walencewicz-Wasserman, A. J.; Kosmoski, J.; Cribbs, D. H.; Glabe, C. G.; Cotman, C. W. *J. Neurochem.* **1995**, *64*, 253–265.

(4) Iversen, L. L.; Mortishire-Smith, R. J.; Pollack, S. J.; Shearman, M. S. *Biochem. J.* **1995**, *311*, 1–16.

(5) Barrow, C. J.; Zagorski, M. G. *Science* **1991**, *253*, 179–182.

(6) Fraser, P. E.; Nguyen, J. T.; Surewicz, W. K.; Kirschner, D. A. *Biophys. J.* **1991**, *60*, 1190–1201.

(7) Hilbich, C.; Kisters-Woike, B.; Reed, J.; Masters, C. L.; Beyreuther, K. *Eur. J. Biochem.* **1991**, *201*, 61–69.

(8) Burdick, D.; Soreghan, B.; Kwon, M.; Kosmoski, J.; Knauer, M.; Henschen, A.; Yates, J.; Cotman, C.; Glabe, C. *J. Biol. Chem.* **1992**, *267*, 546–554.


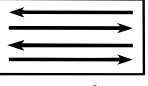


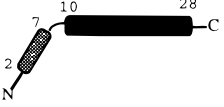
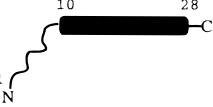
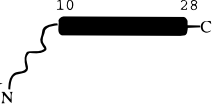






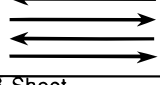


(9) Snyder, S. W.; Ladrör, U. S.; Wade, W. S.; Wang, G. T.; Barrett, L. W.; Matayoshi, E. D.; Huffaker, H. J.; Krafft, G. A.; Holzman, T. F. *Biophys. J.* **1994**, *67*, 1216–1228.

(10) Otvos, L. J.; Szendrei, G. I.; Lee, V. M. Y.; Mantsch, H. H. *Eur. J. Biochem.* **1993**, *211*, 249–257.

(11) Terzi, E.; Hölzemann, G.; Seelig, J. *Biochemistry* **1994**, *33*, 7434–7441.

(12) Marciniowski, K. J.; Shao, H.; Clancy, E. L.; Zagorski, M. G. *J. Am. Chem. Soc.* **1998**, *120*, 11082–11091.

Table 1. Distribution of Solution Structures for the β -(1–28) Peptide^a

Solvent Conditions	Predominate Structure			
	pH 1–4	pH 4–7	pH 7–8	pH 8–12
water	 Random Coil	 Random Coil & β -Sheet	 Random Coil	 Random Coil
SDS-water	 α -Helix (residues 2–7 & 10–28)	 α -Helix (residues 10–28)	 α -Helix (residues 10–28)	 Random Coil
DPC-water	 α -Helix (residues 2–7 & 10–28)	 Random Coil	 Random Coil	 Random Coil
60% TFE-water	 α -Helix (residues 2–7 & 10–28)	 β -Sheet	 α -Helix (residues 10–28)	 α -Helix (residues 10–28)

^a Taken from the previous results.^{12,18,75} The α -helical structure is monomeric and shown with darkened cylinders, while the β -sheet structure is aggregated and antiparallel (arrows in opposite directions)¹⁵.

dissociation constants (pK_a) of the aspartic acid (Asp1, Asp7, Asp23), glutamic acid (Glu3, Glu11, Glu22), histidine (His6, His13, His14), and tyrosine (Tyr10) residues. The pK_a values were obtained under different solution conditions, which included water, 60% TFE (v/v), sodium dodecyl sulfate (SDS), and dodecylphosphocholine (DPC) micelle solutions. Experimental data consisted of 1D and 2D NMR chemical shifts for a peptide fragment comprising residues 1–28 [β -(1–28)] of the naturally occurring β -(1–40) and β -(1–42) peptides. The NMR approach is ideally suited for determining the site-specific pK_a of ionizable side-chain groups of peptides and proteins.

The present results establish that the Glu and His residues have larger pK_a in SDS solution, compared with those in 60% TFE, DPC, and water. These results suggest that electrostatic interactions are important for both α -helix stabilization and preventing the formation of the amyloid-like β -sheet structure. In SDS, complete loss of the α -helix occurs above pH 7.8, which corresponds to the pK_a of the His13 and His14 residues. Below pH 7.8, the His side chains are predominantly positively charged and bind strongly with the negatively charged SDS surface. Mechanisms are put forth to account for the pH-induced variations in structures, which primarily involve interactions among the charged side chains, the micelle surface, and the α -helix macrodipole.

Results

Preliminary Considerations. The β -(1–28) is an appropriate peptide segment for the present study, since it is mostly hydrophilic and contains a high proportion of charged residues (46%) that are responsible for promoting or inhibiting β -aggregation rates in response to environmental variables such as the pH and solvent polarity. It is also less susceptible to aggregation than the natural β -(1–40) and β -(1–42) peptides, indicating the β -(1–28) is a more amenable for solution NMR

studies. Despite its inability to deposit onto preformed plaques,¹³ the β -(1–28) still produces oligomeric β -sheet structures similar to those found in natural amyloid deposits.^{14,15} In addition, the 1–28 region contains key structural features that are important in mediating amyloid fibrillogenesis by electrostatic interactions.^{16,17} The remaining 29–40 or 29–42 regions are devoid of polar and charged amino acid residues and in solution produce almost exclusively oligomeric β -sheet structure that is unaffected by pH and temperature alterations.¹⁸ It is generally thought that the 29–40 or 29–42 regions nucleate and direct folding of the complete β -peptides into the β -amyloid deposits.^{5,8,19,20}

A potential problem is that the organic cosolvent TFE or the micelles (SDS and DPC) can create inaccurate pH measurements, due to liquid junction potential effects at the pH electrode and a reduction in the ionization rate of water.^{21,22} To address these issues, control studies were set up to determine the side-chain pK_a values for the free amino acids Glu, Asp, His, and Tyr in D₂O, SDS, DPC, and 60% TFE. We felt that these studies

(13) Maggio, J. E.; Mantyh, P. W. *Brain Pathol.* **1996**, *6*, 147–162.

(14) Gorévic, P. D.; Castano, E. M.; Sarma, R.; Frangione, B. *Biochem. Biophys. Res. Commun.* **1987**, *147*, 854–862.

(15) Kirschner, D. A.; Inouye, H.; Duffy, L. K.; Sinclair, A.; Lind, M.; Selkoe, D. J. *Proc. Natl. Acad. Sci. U.S.A.* **1987**, *84*, 6953–6957.

(16) Fraser, P. E.; McLachlan, D. R.; Surewicz, W. K.; Mizzen, C. A.; Snow, A. D.; Nguyen, J. T.; Kirschner, D. A. *J. Mol. Biol.* **1994**, *244*, 64–73.

(17) Huang, T. H. J.; Fraser, P. E.; Chakrabartty, A. *J. Mol. Biol.* **1997**, *269*, 214–224.

(18) Barrow, C. J.; Yasuda, A.; Kenny, P. T. M.; Zagorski, M. G. *J. Mol. Biol.* **1992**, *225*, 1075–1093.

(19) Halverson, K.; Fraser, P. E.; Kirschner, D. A.; Lansbury, P. T. *Biochemistry* **1990**, *29*, 2639–2644.

(20) Jarrett, J. T.; Beger, E. P.; Lansbury, P. T. *Biochemistry* **1993**, *32*, 4693–4697.

(21) Frant, M. S. *How to Measure pH in Mixed & Nonaqueous Solutions*; 1995; pp 39–42.

(22) Barbosa, J.; Hernández-Cassou, S.; Sanz-Nebot, V.; Toro, I. *J. Peptide Res.* **1997**, *50*, 14–24.

Table 2. Measured pK_a Values under Different Solution Conditions

control studies ^a	glutamic acid			histidine			aspartic acid		tyrosine	
D ₂ O	4.2 ± 0.1			6.2 ± 0.1			3.4 ± 0.1		10.2 ± 0.1	
SDS	4.4 ± 0.1			6.3 ± 0.1			4.1 ± 0.1		10.2 ± 0.1	
DPC	4.0 ± 0.2			6.3 ± 0.2			3.4 ± 0.1		9.4 ± 0.1	
60% TFE	4.9 ± 0.1			5.6 ± 0.1			3.7 ± 0.2		10.2 ± 0.1	
	Glu3	Glu11	Glu22	His6	His13	His14	Asp1	Asp7	Asp23	Tyr10
β -(1-28) ^b										
D ₂ O	4.5 ± 0.1	4.5 ± 0.1	4.5 ± 0.1	6.5 ± 0.1	6.6 ± 0.1	6.5 ± 0.1	4.3 ± 0.1	4.3 ± 0.2	4.3 ± 0.2	10.4 ± 0.1
SDS	6.2 ± 0.1	5.5 ± 0.1	6.2 ± 0.1	7.1 ± 0.1	7.7 ± 0.1	7.8 ± 0.1	5.6 ± 0.1	5.7 ± 0.1	5.6 ± 0.1	11.1 ± 0.1
DPC	4.4 ± 0.1	4.5 ± 0.1	4.4 ± 0.1	6.4 ± 0.1	6.4 ± 0.1	6.6 ± 0.1	3.8 ± 0.1	N/D	4.9 ± 0.1	10.7 ± 1.4
60% TFE	4.6 ± 0.2	5.3 ± 0.2	5.3 ± 0.2	6.2 ± 0.1	5.7 ± 0.1	5.7 ± 0.1	3.5 ± 0.2	3.7 ± 0.2	3.9 ± 0.2	N/D
β -(1-28)Gln22 ^b										
60% TFE	4.9 ± 0.2	5.1 ± 0.1	N/A	6.1 ± 0.2	6.1 ± 0.2	5.9 ± 0.2	3.0 ± 0.2	3.4 ± 0.2	5.0 ± 0.2	N/D

^a Control samples contained 5 mM aspartic acid, glutamic acid, histidine, and tyrosine in D₂O. ^b Sample of 0.5 mM β -(1-28) or β -(1-28)Gln22 dissolved in the indicated solvent mixture in D₂O. For the β -(1-28), the pK_a of Asp7 in DPC and Tyr10 in 60% TFE could not be determined (N/D) due to NMR spectral overlap.

were appropriate, since the goal of the present work was to determine the ionization states of the β -(1-28) side chains rather than the effect of the micelles or TFE on the pH. The results of these control studies are presented in Table 2.

As shown, the pK_a values of free Glu, Asp, and His are very similar in D₂O, SDS, and DPC solutions, varying at most ± 0.4 . Exceptions occur in 60% TFE, where relative to standard D₂O values, the pK_a of His is reduced (6.0 \rightarrow 5.6) while that for Glu is elevated (4.3 \rightarrow 4.9). Comparable changes of Glu pK_a values in aqueous TFE or other organic solvent mixtures were noted.²³⁻²⁵ Despite these differences, the control studies establish that the solution conditions exert relatively modest effects on the NMR-derived pK_a values.

Determination of the β -(1-28) pK_a from the NMR Data.

In general, the NMR approach involves recording chemical shift data as a function of apparent pH and then fitting the data to sigmoidal curves using the Henderson-Hasselbalch equation. For the present study, 1D and 2D NMR techniques were sufficient to monitor the changes in chemical shifts for the Asp- β CH₂, Glu- γ CH₂, His-2H, His-4H, and Tyr-3,5H signals. Altogether, increases in pH near the pK_a bring about upfield shifts of these NMR resonances.²⁶ At pH 3 \rightarrow 5 the side chains of Asp and Glu deprotonate (COOH \rightarrow COO⁻), while deprotonation of the His side chains (3NH⁺ \rightarrow 3N) occurs at pH 6 \rightarrow 8.^{27,28} Deprotonation of the Tyr10 phenol hydroxyl (OH \rightarrow O⁻) occurs at pH 9 \rightarrow 12 causing an upfield shift of the 3,5-H signals.

Because the sequence-specific NMR assignments for the β -(1-28) in 60% TFE, SDS, and DPC solutions are already known,^{12,29} identification of the Asp- β CH₂, Glu- γ CH₂, His-2H, His-4H, and Tyr-3,5H spin systems was relatively straightforward. A representative full 2D TOCSY spectrum in 60% TFE and expanded regions are presented in Figures 1 and 2, respectively. The expanded plots were obtained at pH 2.4, 3.5, 4.3, and 4.6, and these illustrate the gradual upfield shifts for the Asp- β CH₂ and Glu- γ CH₂ signals with increasing pH. The aromatic Tyr-3,5H, His-2H, and His-4H signals are sufficiently

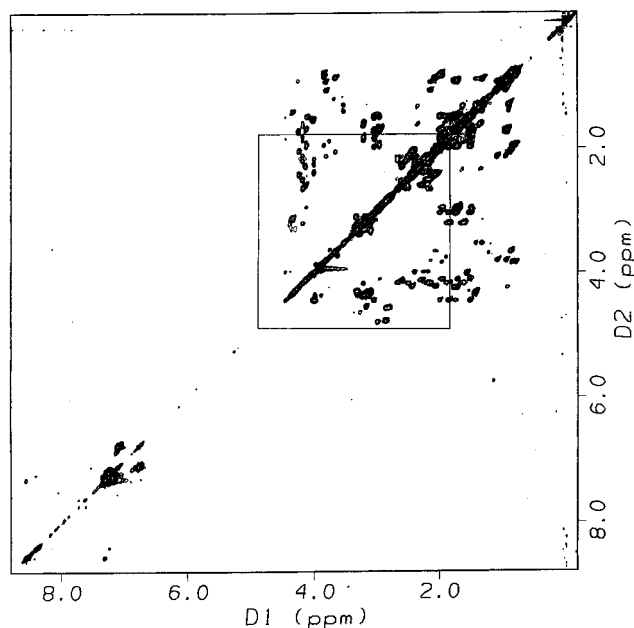


Figure 1. The complete 2D TOCSY spectrum (600 MHz) for 0.5 mM β -(1-28) in 6:4 TFE-D₂O at pH 2.4 and 25 °C. The experiment used a DIPSI-PFG pulse sequence (mixing time 60 ms) and the residual HDO peak was suppressed by presaturation. The boxed-in region shows through-bond direct (two- and three-bond; α H- β H, β H- β H, etc.) and relayed (greater than three bonds) connectivities. Chemical shifts are referenced to internal TSP.

resolved to be followed by 1D methods, so that at neutral and higher pH, 2D spectra were not required. When the predominant conformation for the β -(1-28) was random coil, many NMR signals became degenerate and sequence-specific pK_a determinations were not possible. This situation occurred at pH 1-4 and 7-12 in D₂O, and at pH 4-12 in DPC solutions (Table 1). For example, in D₂O the γ CH₂ signals of Glu3, Glu11, and Glu22 all overlapped, which provided identical pK_a values of 4.5 (Table 2). Graphs showing the variation of chemical shifts with pH for the Glu- γ CH₂, His-2H, and Asp- β CH₂ are depicted in Figure 3 and the computed linear least-squares fit of the NMR data provided the apparent pK_a values (Table 2). A representative comparison of the experimental and computed titration curves for the His-2H in SDS solution is shown in Figure 4. Overall, most of the calculated best fit curves were valid, as reflected by the reported errors (Table 2).

The pK_a values for the Arg5, Lys16, and Lys28 side chains were not determined since their pK_a values are greater than 10,²⁷

(23) Norwood, T. J.; Crawford, D. A.; Steventon, M. E.; Driscoll, P. C.; Campbell, I. D. *Biochemistry* **1992**, *31*, 6285-6290.

(24) Assadi-Porter, F. M.; Fillingame, R. H. *Biochemistry* **1995**, *34*, 16186-16193.

(25) Luo, P.; Baldwin, R. L. *Biochemistry* **1997**, *36*, 8413-8421.

(26) Bundi, A.; Wüthrich, K. *Biopolymers* **1979**, *18*, 285-297.

(27) Cantor, C. R.; Schimmel, P. R. *Biophysical Chemistry: Part I, The Conformation of Biological Macromolecules*; W. H. Freeman: New York, 1980.

(28) Shoemaker, K. R.; Kim, P. S.; York, E. J.; Stewart, J. M.; Baldwin, R. L. *Nature* **1987**, *326*, 563-567.

(29) Zagorski, M. G.; Barrow, C. J. *Biochemistry* **1992**, *31*, 5621-5631.

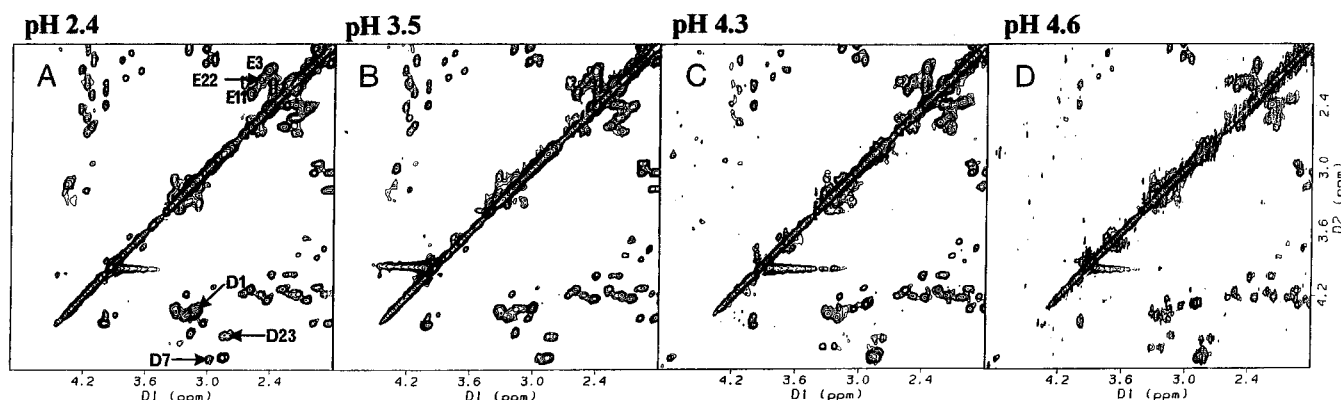


Figure 2. Expanded aliphatic TOCSY region for the β -(1–28) (0.5 mM) in 6:4 TFE–D₂O at 25 °C. The spectra were obtained at pH 2.4 (A), 3.5 (B), 4.3 (C), and 4.6 (D), in which the spectrum at pH 2.4 corresponds to the boxed-in region of Figure 1. These spectra illustrate the gradual upfield shifts for the Asp- β CH₂ and Glu- γ CH₂ signals with increasing pH.

which is in a range where structural variation does not occur (Table 1). As discussed before, at pH 4–7 significant structure rearrangements can take place, establishing the importance of the Asp, Glu, and His side chains in β -amyloid formation.

Repeating the measurements with 1 M NaCl did not significantly alter the pK_a values (± 0.2), suggesting that the Glu, Asp, and His side chains do not form salt bridges. Above pH 4, the two Glu- γ -CH₂ protons were chemically shift equivalent, while below pH 3 their chemical shifts often differed up to 0.09 ppm.^{12,29} Again, these results are consistent with the absence of salt-bridge interactions and solvent-exposed side chains. When unprotonated, the Glu-CH₂-CH₂-COO[−] has complete rotational freedom, consistent with no backbone hydrogen bonding and the chemical shift equivalence. Nearly identical His and Asp pK_a values were obtained by monitoring the chemical shifts of either the His-2H or His-4H, as well as either of the diastereotopic Asp- β CH₂ signals, respectively, thus establishing uniformity of the NMR data.

An important issue is whether the observed pH-dependent chemical shifts originate solely from protonation/deprotonation or also from conformational changes of the β -(1–28). For globular proteins, a prerequisite for pK_a measurements by NMR is that protein should have the same three-dimensional structure within the pH ranges needed to measure the pK_a . Our previous NMR studies of the β -(1–28) indicated that the β -sheet structure is NMR invisible, due to the rapid interconversions among the different sized aggregates as well as the subsequent precipitation. Therefore, during the α -helix \rightarrow β -sheet and random coil \rightarrow β -sheet conversions, only the α -helix and random coil structures are NMR detectable,²⁹ which suggests that the β -(1–28) conformational conversions should not affect the chemical shifts or the pK_a . To confirm this interpretation, additional control experiments were undertaken to explore the effects of conformational rearrangements on the chemical shifts and the pK_a .

For this control project, we determined the Asp, Glu, and His pK_a values for a mutant β -(1–28)Gln22 peptide that contains glutamine (Gln) at position 22 instead of Glu. This mutation is associated with hereditary cerebral hemorrhage with amyloidosis-Dutch type (HCHWA-D), which is a disease (analogous to AD) characterized by extensive amyloid deposition within the cerebral arterioles.^{30,31} The β -(1–28)Gln22 adopts a stable structure over a wide pH range, and therefore is

a useful prototype for comparison with the wild type β -(1–28) (Vassilev and Zagorski, unpublished results). Unlike the wild type β -(1–28) peptide, which undergoes a conformational rearrangement (α -helix \rightarrow β -sheet) at pH 4–7 in 60% TFE (Table 1), the β -(1–28)Gln22 adopts a stable α -helix within the Tyr10-Lys28 region at pH 1–12.

The pK_a for the β -(1–28)Gln22 were determined in an analogous manner as done with the β -(1–28). As shown in Table 2, the Glu and His pK_a values for the β -(1–28) and β -(1–28)Gln22 are very similar (± 0.4). The only major difference is with Asp23, which has an elevated pK_a (3.9 \rightarrow 5.0) for the β -(1–28)Gln22. This may be due to its location near the negatively charged C-terminal pole of the α -helix macrodipole.²⁹ Overall, the lack of any other major differences between the β -(1–28) and β -(1–28)Gln22 pK_a values establishes that the conformational changes do not significantly affect the chemical shifts, in support of our previous conclusions.

Discussion

In solution, the amyloid β -peptide exists as a dynamic ensemble of rapidly interconverting structures, some at equilibrium while others such as the β -amyloid deposit representing an end point. The intention of the present study was to provide site-specific information about the pH-induced structural changes and the role of electrostatics in β -amyloidosis.

Relationships Surrounding the pK_a , Solution Conditions, and Structures. Several complications can occur with pK_a determination of peptides and proteins from NMR data.³² The chemical shift for a given NMR resonance reflects an average value for all titrating groups (protonated and nonprotonated), as well as the averaging of two or more different conformational states that may be in rapid equilibrium. Additionally, for a given conformation the microenvironment around each side chain can be different, such as the electrostatic interactions from neighboring ionizable groups and the heterogeneous dielectric environment in the protein, all of which can affect the pK_a . However, most of these inherent problems occur with large, globular proteins, where multiple titrating groups can influence each other from long-range interactions within the protein interior. These groups usually produce titration curves that are difficult to interpret in terms of a single pK_a value. Fortunately, with relatively small peptides, such as the β -(1–28), these long-range interactions are absent and the side chains are predominantly isolated and in solvent-accessible states. Unlike the hydrophobic

(30) Haan, J.; Roos, R. A. C.; Briet, P. E.; Herpers, M. J. H. M.; Luyendijk, W.; Bots, G. T. A. M. *Clin. Neurol. Neurosurg.* **1989**, 91–4, 285–290.

(31) Levy, E.; Carman, M. *Science* **1990**, 248, 1124–1126.

(32) Forman-Kay, J. D.; Clore, G. M.; Gronenborn, A. M. *Biochemistry* **1992**, 31, 3442–3452.

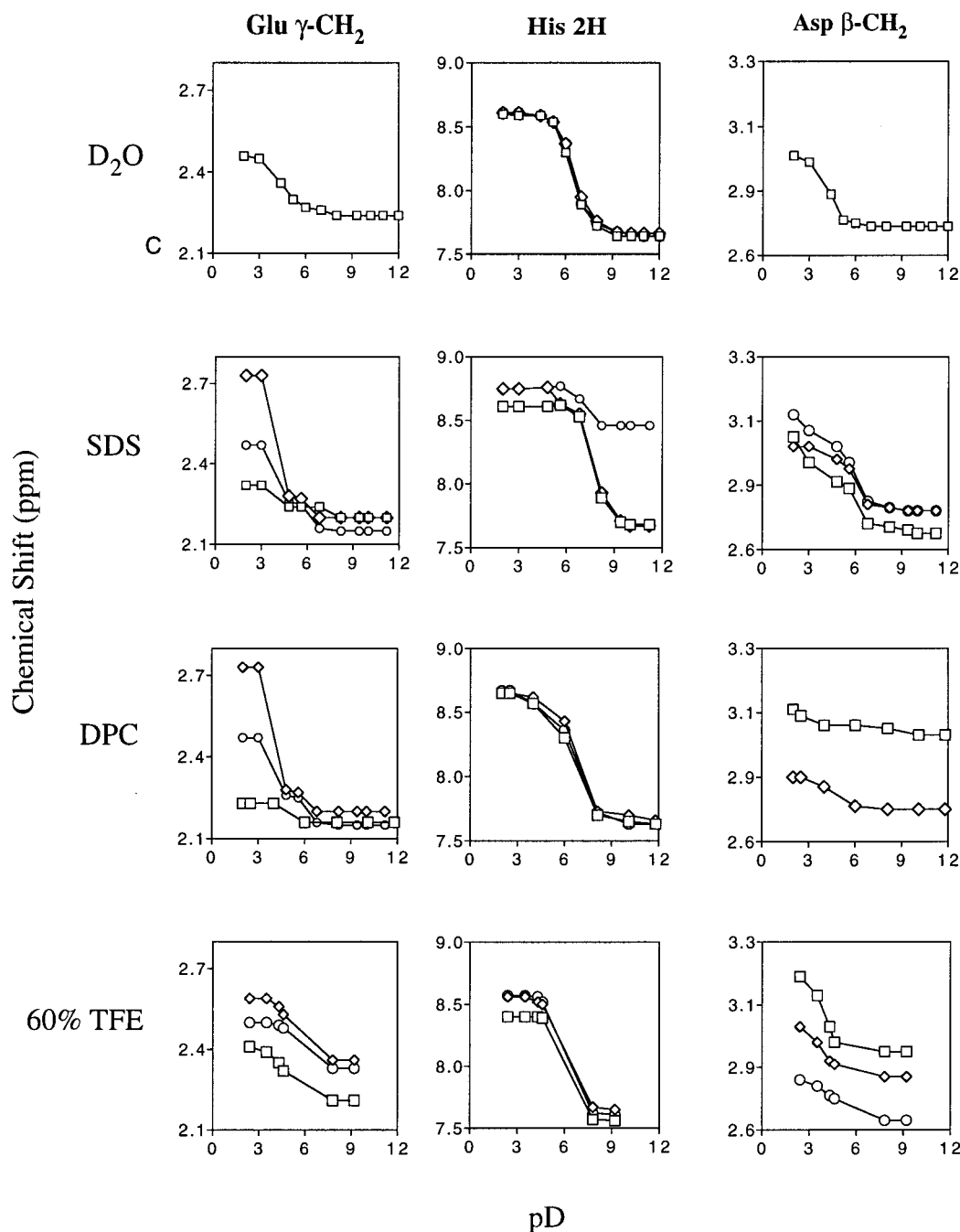


Figure 3. Graphical representation of the pD dependence of the chemical shifts for the Glu γ -CH₂, His-2H, and Asp β -CH₂ of the β -(1-28). The plots for the Tyr10 3,5H are not included. The solvent conditions shown at the left are described in more detail in the text. The secondary structures for each condition are summarized in Table 1. The points for Glu3, His6, and Asp1 are shown with diamonds; Glu11, His13, and Asp7 with circles; and His14, Glu22, and Asp23 with squares.

interior of a globular protein, when the β -(1-28) is folded as an α -helix or in a random coil conformation, the side chains are solvent accessible. Our control study of the β -(1-28)Gln22 reinforced this conclusion, in that the conformational rearrangements (random coil \rightarrow β -sheet and α -helix \rightarrow β -sheet) do not greatly influence the pK_a (Table 2). Moreover, the three-dimensional structures of the β -(1-28) and β -(1-28)Gln22 peptides are virtually indistinguishable at acidic and basic pH (i.e., predominantly random coil in water and α -helical in 60% TFE), which further establishes that other charged groups in the microenvironment do not contribute to either the chemical shift changes or the pK_a .

In general, the β -(1-28) pK_a values are slightly elevated relative to those for the free amino acids (Table 2), which are within

the expected range of 1 pH unit when comparing side chains of proteins and free amino acids.²⁷ A more prominent elevation takes place in DPC solution, where the Asp23 pK_a is 1.5 units higher. This effect may be the consequence of the accompanying α -helix \rightarrow random coil conversion that occurs within the pH 4–5 range (Table 1). Since the Asp23 has a higher pK_a value relative to the other Asp and Glu residues, its side chain probably dissociates immediately before the α -helix \rightarrow random coil conversion. In DPC at pH > 4, the β -(1-28) is predominantly random coil allowing the His side chains greater access to solvent molecules (Table 1), which is reflected in their more normal pK_a values (0.1–0.3 units greater than the free amino acid).

In D₂O at pH 1–4.5 and 6.6–12, the β -(1-28) is monomeric and predominantly in extended forms based on the His pK_a 6.5–

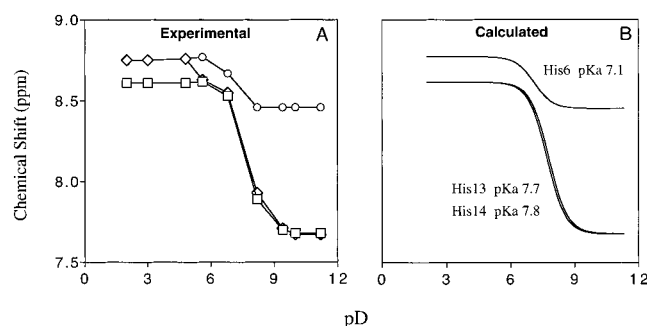


Figure 4. Representative titration curves for the His6 (circles), His13 (diamonds), and His14 (squares) in SDS solution showing the pD dependence of the His-2H chemical shifts. Shown are both the raw experimental data curves (A) and the calculated best fit curves (B) that were fit to an ideal titration curve.

6.6, Glu pK_a 4.3, and Asp pK_a 4.5. Thus, β -aggregation is probably maximized at pH 4.5–6.6, where the Glu, Asp, and His side chains are all charged, in accordance with reports showing that the aggregated β -sheet structure is stabilized by intermolecular ion-pairing interactions.^{16,17}

In 60% TFE at pH 1–4 and 7–12, the backbone is largely α -helical causing the side chains to adopt more pronounced nonrandom spatial arrangements.^{33,34} The organic solvent TFE lowers the His and raises the Glu pK_a values (Table 2). Similar elevations of Glu pK_a values in aqueous TFE or other organic solvent mixtures were noted,^{23–25} and these were partly attributed to the lower dielectric constant of TFE (1/3 that of water). However, the formation of predominantly β -sheet structure in both water and 60% TFE at midrange pH 4–7 establishes that structure formation and aggregation are not due exclusively to dielectric effects. This interpretation is consistent with studies of the pH-dependent stability of ribonuclease A S-peptide.³⁵ It is also possible that the TFE binds to the Glu and His side chains,^{22,36} and the bound TFE may be less capable of stabilizing the charged Glu-COO[−] or His-NH⁺ by solvation. This conclusion is supported by reports that TFE stabilizes α -helices by binding or interacting directly with the charged peptide surfaces.^{36,37}

Micelle Binding Prevents β -Sheet Formation. For the β -(1–28), the data in SDS solution shows that the pK_a values for the Glu, Asp, and His are all significantly higher, by about 1.1–1.6 units relative to the free amino acids (Table 2). Such large increases cannot be solely attributed to reduced solvations and most likely also involve electrostatic contributions. Similar conclusions were reached with other peptides and proteins, in which comparable pK_a elevations occurred in SDS solutions.^{38–42} More recently, the β -(1–40) in SDS solution likewise had higher pK_a values for the Glu22 and Asp23 (pK_a in the 6–7 range),⁴³ consistent with the present data of the β -(1–28).

Shown in Figure 5 is a proposed mechanism for the association of the β -(1–28) with the SDS micelle. Our previous NMR data revealed that, when folded as an α -helix, the β -(1–28), β -(1–40), and β -(1–42) peptides associate at the lipid/water interface, rather than within the hydrophobic SDS micelle

interior.^{12,44} The present pK_a data support this interpretation, in which the highly negatively charged environment around the SDS surface hinders both the deprotonation of the HisNH⁺ and generation of the negatively charged Asp-COO[−] and Glu-COO[−]. An internal location of these side chains would not be consistent with the higher pK_a constants. The His6 side chain has a slightly lower pK_a (7.1), relative to His13 (pK_a 7.7) and His14 (pK_a 7.8). This may result from the greater side-chain mobility of His6, which is within a disordered region while His13 and His14 are within an α -helix (Table 1). Once the His13 and His14 side chains deprotonate, the α -helix breaks down generating random-coil structure. This process is reversible, since reductions in pH below 8 regenerate the α -helix.¹²

With the exception of the Asp residues, the β -(1–28) pK_a values in D₂O and DPC are nearly identical (± 0.2), consistent with solvent-exposed side chains (random-coil structure), and weak hydrophobic interactions between the β -(1–28) and the neutral DPC micelle. However, at pH 4–7 the β -sheet structure forms in D₂O solution, but not in D₂O containing DPC (Table 1). The lack of β -sheet in DPC solution suggests that hydrophobic interactions may be important for preventing the β -sheet formation. Because in water solution the Phe19 and Phe20 residues are important for promoting β -sheet structure,^{45–49} one possibility is that these residues interact weakly with the hydrophobic chains of the DPC micelle in a manner that prevents intermolecular β -aggregation.¹²

In summary, both electrostatic and hydrophobic interactions between the β -(1–28) and the negatively charged shell of SDS and the hydrophobic chains of the DPC micelles, respectively, prevent β -sheet aggregation. These interactions are not possible in D₂O and 60% TFE and, as a result, β -sheet aggregation occurs at midrange pH 4–7 (Table 1).

Mechanism of the pH-Induced α -Helix \rightarrow β -Sheet Rearrangement. Interactions of charged side-chain groups to form salt bridges or with the α -helix macrodipole are important factors affecting α -helix stability.^{28,50–53} The salt-bridge interactions could involve intramolecular Glu- -His or Asp- -His that might contribute to α -helix formation.^{54–56} However, because salt bridges would be expected to form when both the side chains are charged at pH 4–7, they are not likely involved with α -helix formation at pH 1–4 or 7–10. Instead, salt bridging is important

(38) Wu, C.-S. C.; Ikeda, K.; Yang, J. T. *Biochemistry* **1981**, *20*, 566–570.

(39) Woolley, G. A.; Deber, C. M. *Biopolymers* **1987**, *26*, S109–S121.

(40) Henry, G. D.; Sykes, B. D. *Methods Enzymol.* **1994**, *239*, 520–534.

(41) Van Den Hooven, H. W.; Spronk, C. A. E. M.; Van De Kamp, M.; Konings, R. N. H.; Hilbers, C. W.; Van De Ven, F. J. M. *Eur. J. Biochem.* **1996**, *235*, 394–403.

(42) Keire, D. A.; Fletcher, T. G. *Biophys. J.* **1996**, *70*, 1716–1727.

(43) Coles, M.; Bicknell, W.; Watson, A. A.; Fairlie, D. P.; Craik, D. J. *Biochemistry* **1998**, *37*, 11064–77.

(44) Shao, H.; Jao, S.-C.; Ma, K.; Zagorski, M. G. *J. Mol. Biol.* **1999**, *285*, 755–773.

(45) Hilbich, C.; Kisters-Woike, B.; Reed, J.; Masters, C. L.; Beyreuther, K. *J. Mol. Biol.* **1992**, *228*, 4609–473.

(46) Lorenzo, A.; Matsudaira, P.; Yankner, B. A. *Soc. Neurosci. Abstr.* **1993**, *19*, 184.

(47) Esler, W. P.; Stimson, E. R.; Ghilardi, J. R.; Lu, Y.-A.; Felix, A. M.; Vinters, H. V.; Mantyh, P. W.; Lee, J. P.; Maggio, J. E. *Biochemistry* **1996**, *35*, 13914–13921.

(48) Zhang, S.; Casey, N.; Lee, J. P. *Fold Des.* **1998**, *3*, 413–22.

(49) El-Agnaf, O. M.; Guthrie, D. J.; Walsh, D. M.; Irvine, G. B. *Eur. J. Biochem.* **1998**, *256*, 560–9.

(50) Kim, P. S.; Baldwin, R. L. *Annu. Rev. Biochem.* **1990**, *59*, 631–660.

(51) Bradley, E. K.; Thomason, J. F.; Cohen, F. E.; Kosen, P. A.; Kuntz, I. D. *J. Mol. Biol.* **1990**, *215*, 607–622.

(52) Muñoz, V.; Serrano, L. *J. Mol. Biol.* **1995**, *245*, 275–296.

(53) Jones, S.; Thornton, J. M. *Prog. Biophys. Mol. Biol.* **1995**, *63*, 31–65.

(33) Talafous, J.; Marcinowski, K. J.; Klopman, G.; Zagorski, M. G. *Biochemistry* **1994**, *33*, 7788–7796.

(34) Sticht, H.; Bayer, P.; Willbold, D.; Dames, S.; Hilbich, C.; Beyreuther, K.; Frank, R. W.; Rösch, P. *Eur. J. Biochem.* **1995**, *233*, 293–298.

(35) Nelson, J. W.; Kallenbach, N. R. *Proteins: Struct. Funct. Genet.* **1986**, *1*, 211–217.

(36) Jasanoff, A.; Fersht, A. R. *Biochemistry* **1994**, *33*, 2129–2135.

(37) Luidens, M. K.; Figge, J.; Breeze, K.; Vajda, S. *Biopolymers* **1996**, *39*, 367–376.

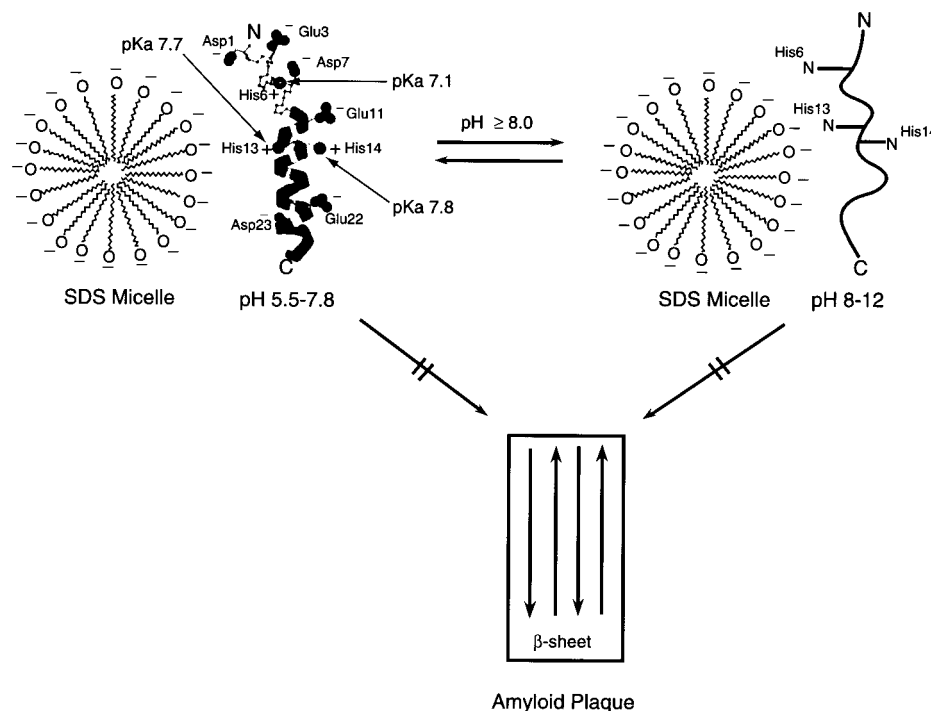


Figure 5. Mechanism for the association of the β -(1–28) with the SDS micelle and the related pH-induced structural changes. Based on 2D NMR,¹² the Tyr10–Lys28 region is α -helical, while the random coil regions are depicted with wavy lines. The α -helical structure corresponds to the actual averaged, energy-minimized NMR-derived tertiary structure of the β -(1–28),³³ in which the helix backbone is drawn with a ribbon and the His-3N, Asp- γ COO, and Glu- δ COO side-chain atoms are shown in their correctly charged state (depending on their pK_a and the external pH). The structures are not scaled according to their true sizes, as the SDS micelle is much larger than the β -(1–28).⁴⁰ This scheme highlights the importance of electrostatic contributions to the α -helix stability. When protonated, the His13 and His14 side chains become bound to the negatively charged SDS surface. Because the His13 and His14 are within the α -helix, they have higher pK_a values than the His6 side chain that is located in an unstructured region (more solvent exposed). The SDS prevents formation of the amyloid-like β -sheet structure, suggesting that both electrostatic and hydrophobic interactions between the micelle and the β -(1–28) may be occurring (see text).

for β -sheet fibril stability,^{15,16,57} since disruption of these salt bridges promotes fibril dissolution.¹⁷ Although high salt concentrations increase aggregation rates,^{9,58} the present data showed that they do not affect the experimental pK_a values for the soluble α -helix and random coil structures. Thus, the α -helix is stabilized by local interactions, whereas the aggregated β -sheet is stabilized by long-range effects such as salt bridges.

Figure 6 depicts a mechanism showing the possible charge-helix macrodipole interactions that could account for the α -helix \rightarrow β -sheet conversion. We had previously proposed that the largest contributors to α -helix destabilization at pH 4–7 are unfavorable interactions between charged amino acid side chains and the α -helix macrodipole.²⁹ The alignment of peptide bonds within an α -helix creates a macrodipole, in which the negative pole is at the C-terminus and the positive pole is at the N-terminus. The field of an α -helix macrodipole is approximately equal to the field of a half positive unit charge at the N-terminus and a half negative unit charge at the C-terminus.⁵⁹ Hence, α -helix formation is favored if one pole of the macrodipole and a nearby charged residue have opposite signs, and oppose α -helix formation if they are of like sign.

These interactions are strongest for charged side chains located within the first and second α -helical turns and long α -helices are not required for significant dipoles.^{60,61} Thus, because Glu11, His13, His14, Glu22, and Asp23 are located within the second turns of the Tyr10–Lys28 α -helix, their ionization states can either reinforce or oppose the helix macrodipole. Because of their longer length, the positively charged side chains of Lys16 and Lys28 are highly solvated and can adopt conformations that reduce interactions with the helix macrodipole.⁵⁹

When His13 and His14 are protonated, an unfavorable charge interaction is possible between the positively charged His side chains and the positively charged N-terminal pole (Figure 6). Likewise, when Glu22 and Asp23 are deprotonated, an unfavorable charge interaction can exist between the negatively charged side chains and the negatively charged C-terminal pole. Only the negatively charged Glu11 has a favorable interaction with the α -helix macrodipole.

Within the Tyr10–Lys28 α -helix, the His13 and His14 protonate at identical values (pK_a 5.7), whereas in the pH 3–6 range, the Asp23 first dissociates (pK_a 3.9) followed by Glu22 (pK_a 5.3) and Glu11 (pK_a 5.3) (Table 2). Remarkably, the Glu11, which has a favorable interaction with the α -helix macrodipole, has an elevated pK_a (5.3) relative to the control studies (4.9). This may be due to a slightly reduced solvation or weak intramolecular hydrogen bonding effects from the nearby positively charged His13 and His14 side chains.⁶² The α -helix \rightarrow β -sheet conversion above pH 4 is not promoted by the Asp23

(54) Marqusee, S.; Baldwin, R. L. *Proc. Natl. Acad. Sci. U.S.A.* **1987**, *84*, 8898–8902.

(55) Yang, A.-S.; Honig, B. *J. Mol. Biol.* **1993**, *231*, 459–474.

(56) Huyghues-Despointes, B. M. P.; Baldwin, R. L. *Biochemistry* **1997**, *36*, 1965–1970.

(57) Lee, J. P.; Stimson, E. R.; Ghilardi, J. R.; Mantyh, P. W.; Lu, Y.-A.; Felix, A. M.; Llanos, W.; Behbin, A.; Cummings, M.; van Crielinge, M.; Timms, W.; Maggio, J. E. *Biochemistry* **1995**, *34*, 5191–5200.

(58) Hilbich, C.; Kisters-Woike, B.; Reed, J.; Masters, C. L.; Beyreuther, K. *J. Mol. Biol.* **1991**, *218*, 149–163.

(59) Spassov, V. Z.; Ladenstein, R.; Karshikoff, A. D. *Protein Sci.* **1997**, *6*, 1190–1196.

(60) Aqvist, J.; Luecke, H.; Quiocho, F. L.; Warshel, A. *Proc. Natl. Acad. Sci. U.S.A.* **1991**, *88*, 2026–2030.

(61) Sitkoff, D.; Lockhart, D. J.; Sharp, K. A.; Honig, B. *Biophys. J.* **1994**, *67*, 2251–2260.

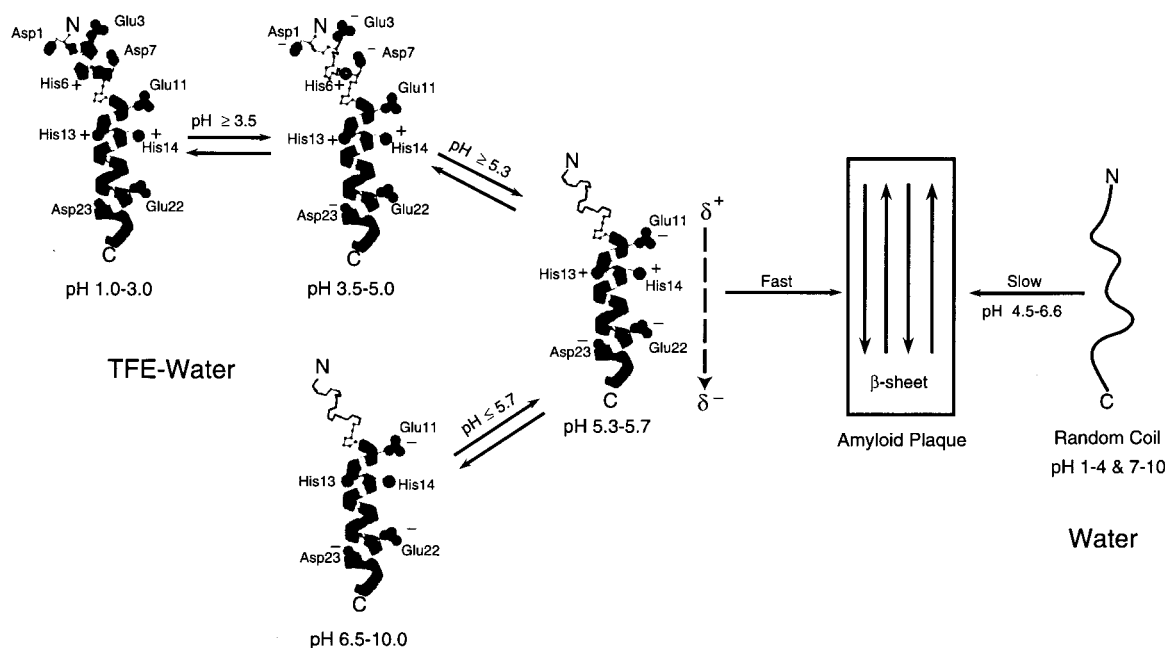


Figure 6. Mechanism for the α -helix \rightarrow β -sheet and random coil \rightarrow β -sheet conversions, which is an extension of our previous model and now includes more specific pH ranges.²⁹ Using the NMR-derived tertiary structure of the β -(1–28),³³ the α -helix backbone is drawn with a ribbon and the His-3N, Asp- γ COO, and Glu- δ COO side-chain atoms are shown in their correctly charged state (depending on the pH and the side-chain pK_a). At acidic pH 1–3, there are two α -helical regions (Ala2–Asp7 and Tyr10–Lys28) while at pH 3.5–5.0 and 6.5–10.0 the shorter α -helix breaks down. When the side chains of Glu11, Glu22, and Asp23 deprotonate (δ COOH \rightarrow δ COO $^-$) above pH 5.3, and the side chains of His13 and His14 protonate ($3NH \rightarrow 3N^+$) below pH 5.7, a rearrangement takes place (α -helix \rightarrow β -sheet). This rearrangement is very rapid and comes about from the unfavorable charged interactions (same sign) between the side chains and the α -helix macrodipole. Since the β -(1–28) is random coil in water solution, a similar α -helix-macrodipole effect is not possible, resulting in a slower aggregation rate.

ionization (pK_a 3.9), but rather by the subsequent ionization of the Glu22 side chain (pK_a 5.3). These results suggest that disruption of the α -helix is caused by the ionization of His13, His14, and Glu22, and their resultant unfavorable charged interactions with the α -helix macrodipole. This hypothesis is supported by our studies with the β -(1–28)Gln22, which does not undergo a related α -helix \rightarrow β -sheet rearrangement at pH 4–7. This greater α -helix stability can be attributed to the absence of the unfavorable interchange between the negatively charged Glu22 and the α -helix macrodipole. The predominantly α -helical structure of the β -(1–28)Gln22 is supported by other NMR studies in dimethyl sulfoxide.⁶³

Additional support for the mechanism outlined in Figure 6 comes from a comparison of the pK_a values within the amino acid types (Table 2). For example, in 60% TFE the Asp23 pK_a is 0.2 and 0.4 units higher than those for Asp7 and Asp1, respectively (Table 2). The higher pK_a for Asp23 can be explained by its location near the C-terminus of the α -helix macrodipole, while the Asp1 and Asp7 have more normal pK_a values (identical or close to the control study); the Asp1 and Asp7 occupy unstructured regions and are not interacting with an α -helix macrodipole (Figure 6). In related studies of other short peptide α -helices, the Asp pK_a values were higher when positioned near the C-terminus relative to the N-terminus.⁶² A similar explanation can explain why the His6 pK_a is 0.5 units higher than His13 and His14, as the His6 is also located in a random coil region. Both the His and Asp residues play important roles in β -amyloid fibril production and stability. Many physiological constituents such as transthyretin and zinc can prevent or promote aggregation by their affinities for the His residues of β -peptide.^{64,65} The His13 residue is important for amyloid fibril assembly and disassembly as a function of pH.⁶ In addition, rat and mice do not develop mature amyloid

deposits in vivo and, in these mammals, β -peptide contains an Arg13 rather than His13.⁶⁶

Conclusions. The present studies are the first to provide residue-specific data about the pH-dependent structural changes of the amyloid β -peptide. The distinct pK_a for the side chains of the His13, His14, and Glu22 imply that these residues possess especially critical roles in the α -helix \rightarrow β -sheet conversion that may be important in AD pathogenesis. The α -helix \rightarrow β -sheet conversion is supported by a mechanism involving unfavorable electrostatic interactions between the α -helix macrodipole and the charged side chains. The Glu and His side chains have elevated pK_a constants in SDS solution, indicating that they are bound to the negatively charged SDS surface. Because both the negatively charged SDS and the neutral DPC prevent β -sheet formation, a weak hydrophobic interaction between the DPC micelle and hydrophobic amino acid residues may be occurring. This idea implies that the charged and polar residues make stronger contacts with negatively charged micelle surfaces, while hydrophobic peptide regions may interact with the neutral micelle lipid chains.

Experimental Section

Peptide Synthesis and Purification. The β -(1–28) peptide was prepared and purified as described previously¹² and its primary amino

(62) Joshi, H. V.; Meier, M. S. *J. Am. Chem. Soc.* **1996**, *118*, 12038–12044.

(63) Sorimachi, K.; Craik, D. J. *Eur. J. Biochem.* **1994**, *219*, 237–251.

(64) Schwarzman, A. L.; Gregori, L.; Vitek, M. P.; Lyubski, S.; Strittmatter, W. J.; Enghilde, J. J.; Bhasin, R.; Silverman, J.; Weisgraber, K. H.; Coyle, P. K.; Zagorski, M. G.; Talafous, J.; Eisenberg, M.; Saunders, A. M.; Roses, A. D.; Goldgaber, D. *Proc. Natl. Acad. Sci. U.S.A.* **1994**, *91*, 8368–8372.

(65) Bush, A. I.; Pettingell, W. H.; Paradis, M. D.; Tanzi, R. E. *J. Biol. Chem.* **1994**, *269*, 12152–12158.

(66) Johnstone, E. M.; M. O., C.; Norris, F. H.; Pascual, R.; Little, S. P. *Mol. Brain Res.* **1991**, *10*, 299–305.

acid sequence is as follows: $\text{H}_3\text{N}^+-\text{D}^1-\text{A}-\text{E}-\text{F}-\text{R}^5-\text{H}-\text{D}-\text{S}-\text{G}-\text{Y}^{10}-\text{E}-\text{V}-\text{H}-\text{H}-\text{Q}^{15}-\text{K}-\text{L}-\text{V}-\text{F}-\text{F}^{20}-\text{A}-\text{E}-\text{D}-\text{V}-\text{G}^{25}-\text{S}-\text{N}-\text{K}-\text{COO}^-$.

Sample Preparation. Perdeuterated SDS- d_{25} , DPC- d_{38} , TFE- d_3 ($\text{CF}_3\text{-CD}_2\text{OD}$), and D_2O were obtained from Isotec, Inc. (Miami, OH) or Cambridge Isotopes, Inc. (Andover, MA). Samples were prepared for NMR measurements by dissolving the β -(1–28) (0.9 mg, 0.25 μmol , 0.5 mM) in a solution (0.5 mL) of D_2O , TFE- d_3 - D_2O (6:4, v/v), SDS- d_{25} (120 mM) in D_2O , or DPC- d_{38} (120 mM) in D_2O . For the latter two solutions, the SDS and DPC quantities were intentionally set well above their critical micelle concentrations and their average aggregation numbers.⁴⁰ This ensured that at least one micelle molecule was present per molecule of β -(1–28). All solutions also contained trace amounts of sodium 3-(trimethylsilyl)propionate-2,2,3,3- d_4 (TSP), 0.5 mM Na_2EDTA (removes trace metal contaminants), and 0.05 mM NaN_3 (prevents microbial growth).

The three control solutions (0.5 mL) were prepared by dissolving L-tyrosine (0.45 mg, 2.5 μmol , 5.0 mM), L-aspartic acid (0.33 mg, 2.5 μmol , 5.0 mM), L-histidine (0.39 mg, 2.5 μmol , 5.0 mM), and L-glutamic acid (0.37 mg, 2.5 μmol , 5.0 mM) in SDS (120 mM) in D_2O , DPC (120 mM) in D_2O , and TFE- d_3 - D_2O (6:4, v/v). These three solutions were placed into three, 5 mm NMR tubes and the pH measurements and adjustments were done as described above for the β -(1–28) peptide. The amino acids were obtained in 98–99% purity levels (Aldrich, Inc.), and the solutions also contained trace amounts of TSP, 0.5 mM Na_2EDTA , and 0.05 mM NaN_3 .

The pH values were measured with a pH meter (Corning 340) equipped with an electrode (Model MI-412, Microelectrodes, Inc.) that was calibrated with pH 4.00, 7.00, and 12.00 buffers. Similar pH readings were obtained with an Accumet combination glass electrode (pH range 0–14) that used a Calomel reference (Fisher, Inc.). The desired apparent pD values were obtained at room temperature by adding microliter amounts of dilute DCl or NaOD. The pH-meter reading is approximately 0.40 pH units lower in D_2O than in H_2O , suggesting that a correction may be needed.⁶⁷ However, since the isotope effects on glass electrodes and the measured pK_a values of proteins nearly invalidate each other,²⁶ corrections for pH-induced isotope effects were not required. After corrections for temperature, we estimate that the pH readings are accurate ± 0.1 . Readjustments of the pH for the effects of TFE were not performed, since previous studies showed that TFE has only minor effects (± 0.07 units) on the apparent pH.²⁹

To address the potential problems related to the time-dependent structure and aggregation changes at pH 4–7,^{5,6,8} for the studies in D_2O and TFE- d_3 - D_2O (6:4, v/v), two peptide solutions were prepared, one at low pH and the other at high pH, where time-dependent structural changes did not occur. This involved dividing a β -(1–28) solution (1 mL, 0.5 mM) into two equal portions that were placed separately into two, 5 mm NMR tubes. The pH was adjusted to approximately 2–3 and 10–12 for the two solutions. The NMR spectra were recorded within 10 min after the pH adjustment, and thereafter the pH was increased or decreased for the low and high pH solutions, respectively. The pH was obtained prior to NMR measurements and then remeasured after the experiments were completed to ensure that it remained constant during the data acquisition; the two readings usually agreed to within ± 0.05 pH unit. For the NMR measurements in SDS and DPC solutions, one β -(1–28) solution was prepared, since the time-dependent variations do not occur.¹²

NMR Measurements. The NMR spectra were obtained with either a Bruker AMX-2 500 MHz or a Varian Inova-600 MHz spectrometer. The NMR data were transferred to Indigo XS24 computer workstations (Silicon Graphics, Inc.) and processed using the FELIX program (version 95, Biosym, Inc.). Chemical shifts were referenced to an internal standard of TSP and probe temperatures were calibrated using neat methanol.⁶⁸ All measurements were conducted at 25.0 °C. Control experiments using a sample of TSP and dioxane (as a reference) showed minimal chemical shift variations (± 0.01 ppm) of the TSP signal with alterations in pH, indicating that chemical shift corrections for TSP were not required.^{69,70}

The carrier was placed near the center of the spectrum at the position of the residual protium absorption of D_2O (HDO). The HDO signal was suppressed by low-power irradiation during the recycle delay. For 1D NMR spectra, 64 scans were acquired with a total recycle delay of 4.5 s, which included an acquisition time and recycle delay of 2.5 and 2.0 s, respectively. Typically, the digital resolution of the acquired data was 0.20 Hz/pt, which was reduced to 0.10 Hz/pt by zero-filling the data once before processing. Before Fourier transformation, spectra were multiplied by either exponential line broadening or Lorentzian-to-Gaussian weighting factors.

For the 2D homonuclear Hartmann–Hahn or total-correlation spectroscopy (TOCSY),^{71,72} suppression of the HDO signal was done by presaturation. Depending on the signal-to-noise, the NMR data were apodized by a skewed sine-bell squared or exponential line broadening window functions in F_2 and 90° sine-bell squared in F_1 . The TOCSY employed a DIPSI pulse sequence⁷³ with a mixing time of 70 ms, and two trim pulses located at the beginning and end of the DIPSI sequence. Acquisition parameters included 5050 and 6600 Hz sweep widths for the 500 and 600 MHz instruments, with 4096 and 256 complex points (each consisting of 32 scans) for the F_2 and F_1 dimensions, respectively. Usually 2–4 dummy scans were used for each increment and the relaxation delay was set to 1.5 s. After zero-filling in F_1 , the final 2D matrices contained 2048×2048 points.

Apparent pK_a Determinations. The pK_a values were determined by simulating the pH and chemical shift data to the Henderson–Hasselbalch equation,^{26,74} assuming that the pK_a values are independent.³² For peptides and proteins, the shapes of the titration curves are logarithmic expressions of the pK_a (Figure 3), according to the following equation:

$$\text{pK}_a = \text{pH} + \log[(\delta_h - \delta_{\text{exp}})/(\delta_{\text{exp}} - \delta_l)]$$

where δ_{exp} , δ_h , and δ_l are experimental chemical shifts and the individual chemical shifts at high and low pH values, respectively. Using a computer program (kindly provided by Dr. Milo Westler, NMRFAM, University of Wisconsin-Madison) and a nonlinear least-squares method, the experimental data were fit to an ideal titration curve that corresponded to the titration of each individual side chain (for example, see the experimental and ideal titration curves in Figure 4). From the ideal curves, the pK_a values were obtained using the above equation and the computer program. Typically, the single titration curves employed a Hill coefficient set to unity. Error limits are reported from the convergence inaccuracies obtained from the program (differences between the experimental and ideal curves), which also incorporated the uncertainties in the measured chemical shifts and the pH.

Acknowledgment. Supported in part by grants from the American Federation of Aging Research, the National Institutes of Aging (AG-08992-06 and AG-14363-01), a Claire Boothe Luce Graduate Fellowship (E.L.C.), Philip Morris, Inc., and a Faculty Scholars Award from the Alzheimer's Association (M.G.Z.). The 600 MHz NMR spectrometer was purchased with funds provided by the National Science Foundation, the National Institutes of Health, and the Ohio Board of Regents. We would like to thank Milo Westler (NMRFAM, University of Wisconsin-Madison), Haiyan Shao, and Anita Hong (Anaspec, Inc.) for helpful discussions.

JA990864O

(69) De Marco, A. J. *Magn. Reson.* **1977**, 26, 527–528.

(70) Bundi, A.; Wüthrich, K. *Biopolymers* **1979**, 18, 299–311.

(71) Bax, A.; Davis, D. G. *J. Magn. Reson.* **1985**, 65, 355–360.

(72) Rance, M. J. *Magn. Reson.* **1987**, 74, 557–564.

(73) Shaka, A. J.; Lee, C. J.; Pines, A. *J. Magn. Reson.* **1988**, 77, 274–293.

(74) Caceci, M. S.; Cacheris, W. P. *Byte* **1984**, 9, 340–342.

(75) Shao, H.; Marciniowski, K. J.; Clancy, E. L.; Salomon, A. R.; Zagorski, M. G. *The Solution Structures of the β -Amyloid Peptide Provide a Molecular Approach for the Treatment of Alzheimer's Disease*; Iqbal, K., Winblad, B., Nishimura, T., Takeda, M., Wisniewski, H. M., Eds.; John Wiley & Sons, Ltd.: New York, 1997; pp 729–739.

(67) Primrose, W. U. *Sample Preparation*; Roberts, G. C. K., Ed.; Oxford University Press: Oxford, 1993; pp 7–34.

(68) Van Geet, A. L. *Anal. Chem.* **1970**, 42, 679–680.